Journal of Materials Chemistry C

Giant Current Amplification Induced by Ion Migration in Perovskite Single Crystal Photodetectors

Journal:	*Journal of Materials Chemistry C*
Manuscript ID	TC-ART-05-2018-002334.R1
Article Type:	Paper
Date Submitted by the Author:	25-Jun-2018
Complete List of Authors:	Wu, Ting; University of Tennessee, Materials Science and Engineering Ahmadi, Mahshid; University of Tennessee, Materials Science and Engineering Hu, Bin; The University of Tennessee, Department of Materials Science and Engineering

Giant Current Amplification Induced by Ion Migration in Perovskite Single Crystal Photodetectors

Ting Wu[§], Mahshid Ahmadi[§], Bin Hu*

Joint Institute for Advanced Materials, Department of Materials Science and Engineering, University of Tennessee, Knoxville, Tennessee, 37996, USA

*Corresponding Author: Prof. Bin Hu, bhu@utk.edu

[§] These authors contributed equally

KEYWORDS: organic-inorganic hybrid perovskites, single crystal, photodetector, current amplification, ion migration

TOC GRAPHIC

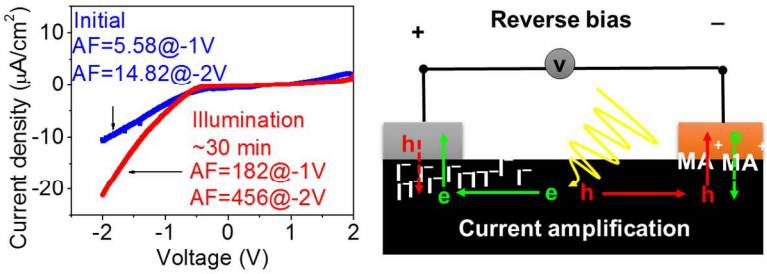
Initial
AF=5.58@-1V
AF=14.82@-2V
Illumination
~30 min
AF=182@-1V
AF=456@-2V
Current density (μA/cm²)
Voltage (V)
Reverse bias
+
–
V
h
e
MA MA
Current amplification

ABSTRACT:

Single crystals of organic-inorganic hybrid perovskites have become attractive candidates for the applications in photodetection and high-energy radiation detection based on unique solution growth with a large interacting cross-section with electromagnetic waves in different energy regimes and high drift mobilities through optically induced polarization. However, the inevitable ion migration often represents a technical difficulty in controlling detection performance. This work reports a giant current amplification induced by ion migration in the $MAPbI_3$ single crystal photodetectors with a lateral geometry of Au/$MAPbI_3$/C_{60}/BCP/Ag based on light soaking studies. Upon light soaking, a stabilized device can demonstrate a giant amplification factor reaching 600 at -2 V under weak light illumination (1 mW/cm^2). The time-dependent current profile shows a slow response during the amplification under light soaking. This indicates that optically activated ions are driven away from working areas to respective electrodes, leading to the reduction of dark current by decreasing bulk defects. Simultaneously, the accumulation of iodine anions and methylammonium cations at Ag and Au contacts can trigger the counter charge injection, largely amplifying the total electrical current and leading to a giant current amplification in perovskite single crystal photodetectors.

Organic-inorganic hybrid perovskites have received intensive interests due to their promising optical and electrical properties for developing multi-functionality, including photovoltaics,[1-4] light-emitting diodes,[5-8] optically pumped lasers,[9-12] photodetection,[13-,,20] and high energy radiation detection[21-,,24]. Since 2015, the single crystals of hybrid perovskites,[25-28] with much more promising properties with respect to its polycrystalline counterpart, have demonstrated a great of advantages for photodetection[16-19] and high energy radiation detection[21-24]. Despite these remarkable achievements in perovskite detectors, it still lacks fundamental understanding on the development of photodetection actions. Particularly, hybrid perovskites are known to possess dual conduction channels, electronic conduction, and ionic conduction.[29-,,32] The ionic conducting characters are highly associated with the operation stability of perovskite optoelectronic devices.[33] Meanwhile, ion migration due to photoexcitation[34,35] or electrical poling[36,37] is known to be one of the origins for the hysteresis effect in perovskite solar cells.[38-,,41] Recently, we found that the mobile ions can interact with metal contacts and leads to interface modified semiconducting properties in perovskite single crystals.[42] This provides a hypothesis that the ion migration can provide a mechanism to trigger the electrical injection and consequently generates a current amplification in perovskite photodetectors.

In this work, we report a giant current amplification in the lateral perovskite single crystal photodetectors, which can be attributed to the effect of ion migration and accumulation with the aid of external bias and photoexcitation. We find that a stabilized device through light soaking for 30 min can generate a giant amplification with amplification factor reaching 600 at -2 V under weak light illumination (1 mW/cm^2). We propose that the giant current amplification in our devices can be attributed to photoexcitation and electrical field induced migration and accumulation of iodine anions (I^-) and methylammonium cations (MA^+) at respective contacts.

The interfacial charging due to ion accumulation offers an effective mechanism to trigger counter charge injection, consequently amplifying the total electrical current. Simultaneously, the field-induced ion migration wipes the defects from the working area to the electrode contacts, leading to the reduction of dark current due to the reduced density of defects within the working area.

RESULTS AND DISCUSSION

The single crystals of $MAPbI_3$, as shown in **Figure 1a**, were grown by a solution growth method reported in our previous publication.[42] By controlling the precursor concentration, oil bath temperature, and cooling rates, we are able to grow large crystals with thickness about 3 mm. The details of single crystal growth can be found in our previous publication.[42] In this study, single crystals with thickness of about 3 mm ensure a large crystal surface (3mm × 3mm) assigned to {100} facet to pattern charge transport layers (C_{60}/BCP) and metal contacts laterally. **Figure 1b** shows the device structure of the single crystal photodetectors with a lateral geometry of Au/$MAPbI_3$/C_{60}/BCP/Ag. The cathode and anode contacts were deposited on the crystal surface with a separation distance of 100 μm by a shadow mask. More specifically, fullerene (C_{60}), and 2,9-Dimethyl-4,7-diphenyl-1,10-phenanthroline (BCP) were sequentially deposited as the electron transport layer, while silver (Ag) and gold (Au) were deposited as cathode and anode contacts, respectively.

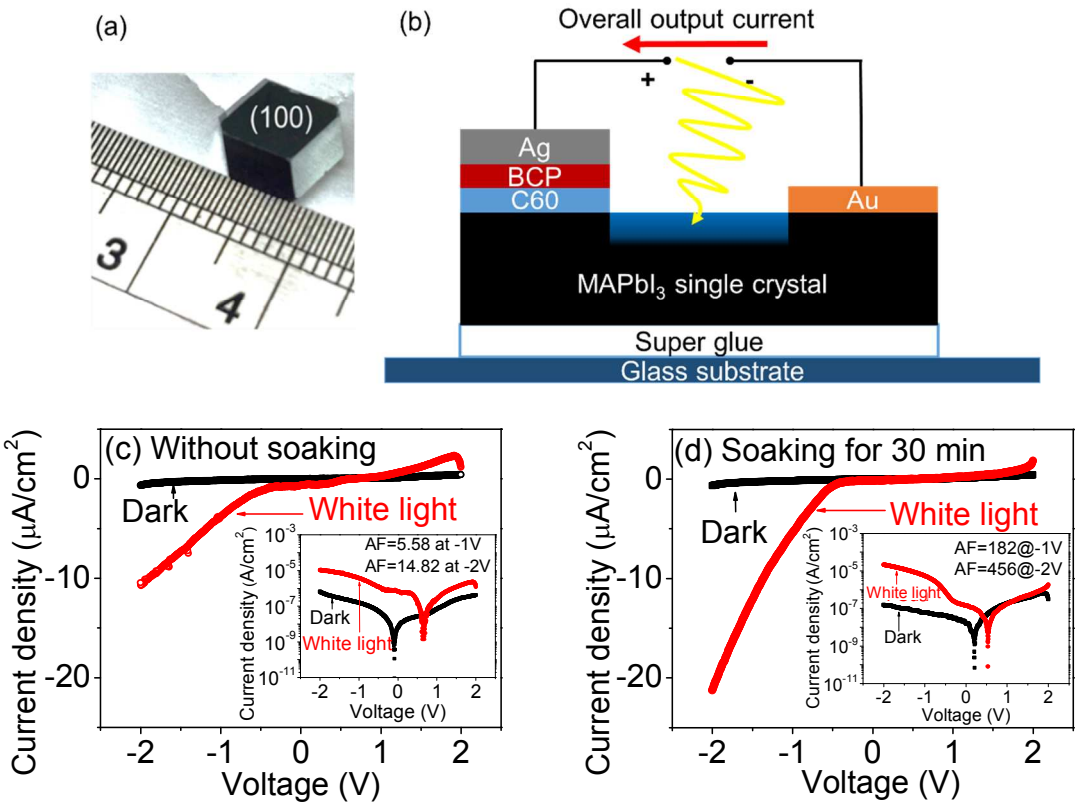

Figure 1. Giant current amplification from $MAPbI_3$ single crystal photodetectors. (a) Photograph of a grown single crystal of $MAPbI_3$. **(b)** Schematic diagram of a photodetector device based on a $MAPbI_3$ single crystal with a lateral geometry; **(c)** Current density-voltage (*JV*) characteristics of the device without soaking in both dark condition and under white light illumination, the inset shows characteristics in semi-logarithm scale and the current amplification factor (AF) at -1 V and -2 V; **(d)** *JV* characteristics in both dark condition and under white light illumination after a light soaking treatment for 30 min, the inset shows the inset shows characteristics in semi-logarithm scale and AF at -1 V and -2 V.

Interestingly, the device exhibits a giant current amplification under electrical biasing and light soaking. The current density-voltage (*JV*) characteristics under both dark condition and white light illumination are shown in **Figure 1c**. The *JV* curve under illumination can be divided into two regimes: (i) photovoltaic (PV) regime at forward bias, and (ii) photodetector (PD) regime at reverse bias. In the PV regime, the device generates an open-circuit voltage (V_{oc}) of

0.68 V, and fill-factor (FF) reaching 40%, but the power conversion efficiency is seriously limited by the inefficient generation of photocurrent under zero bias. However, in the PD regime, we can observe a large current amplification from the lateral single crystal device. In particular, the current under 2 V reverse bias is 0.62 μA/cm^2 in dark condition, but dramatically increases to 10.70 μA/cm^2 under illumination, while the short-circuit current is 0.66 μA/cm^2. This result indicates that the lateral single crystal photodetectors can present a large current amplification effect, in which current amplification factor (AF) is defined by eq 1:[56]

$$\mathrm{AF}=\frac{J-J_{DK}}{J_{SC}} \quad (1)$$

where J is measured electrical current at a given bias, J_{DK} is dark current under the same bias, and J_{SC} is the short-circuit current under the same illumination conditions. The lateral single crystal photodetector gives an AF of 6 and 15 under 1 V and 2 V reverse biases, respectively. The current amplification capability is comparable with the reported values from polycrystalline perovskite photodetectors[56]. More interestingly, when the device is continuously illuminated for 30 minutes (mins), the current density in the PD regime is dramatically enhanced (**Figure 1d**) with the current amplification factor increased from 15 to 456 under 2V reverse bias and white light illumination, while the PV performance is significantly decreased. Meanwhile, the dark current is reduced by one order at 2 V reverse bias after light soaking for 30 min. This indicates that the density of defects within the working area is effectively reduced under the working conditions. The reduction in dark current after light soaking is in agreement with recent studies on photoinduced defect density reduction and defect healing by ion migration.[35,43] More interestingly, it is found that the voltage at the drip of dark *JV* curves is shifted from nearly zero to 0.19 V after illumination for 30 mins, while the Voc is reduced from 0.68 V to 0.55 V. The

reduction in Voc suggests that the light soaking causes a large accumulation of ions at the electrode interface enhancing interfacial charge recombination which is deleterious to the performance of device in photovoltaic regime.[44] Light soaking[45] and light-induced self-poling effect[34] have been revealed in the polycrystalline perovskite photovoltaics. The former effect has been attributed to the neutralizing of charged defects, leading to an enhancement of photovoltaic performance with time. While the latter effect has been interpreted by optically activated ion migration driven by photovoltage (also known as open-circuit voltage). In order to ensure the presence of significant injection at negative bias we have calculated the drift photocurrent expected at -2V according to the simple electrical conduction theory shown in eq 2.

$$J_{ph} = en\mu E \quad (2)$$

where e is the Charge of an electron, n is the number of free charges, μ is the mobility of charge carriers and E is the applied electric filed. By considering the applied -2V and built-in potential (Voc), we can estimate the photocurrent J_{ph} under this reverse bias by using J_{SC} developed by built-in potential. Based on eq. (2), $J_{ph} = J_{SC}*(2+\text{Voc}) = 0.26$ μA/cm^2. Obviously, the estimated photocurrent is much less than the observed photocurrent □21 μA/cm^2 at -2 V. This provides an experimental indication that, after light soaking, the ion migration towards respective electrodes can modify the interfacial barrier and trigger the electrical injection at electrode contacts and consequently generates a giant current amplification in the lateral single crystal photodetectors. It was noted that after 30 mins of light soaking devices are stable however, as a result of further light soaking, a serious issue develops due to ion accumulation and devices become unstable. The longer light soaking can cause photocurrent decay since further ion migration can induce an electric field with opposite direction to the built-in electric field which consequently reduces the collection of photogenerated carriers and photocurrent decays.

It is well stablished that ion migration is time, voltage and photoexcitation dependent. Here, we further examined the time-dependent current under different excitation intensities to understand the underlying mechanism responsible for giant amplification induced by light soaking in the single crystal device. **Figure 2a** shows the time-dependent current profiles measured with repeating light-on and light-off cycles at different excitation intensities from 1 mW/cm^2 to 100 mW/cm^2 under four different biases 0V, -1 V, -2 V and +1 V. We can see that the current is much larger under reverse bias as compared to the zero bias and forward bias. As shown in **Figure 2b**, the amplification factor reaches 600 at -2 V reverse bias under weak light illumination (1 mW/cm^2), but decreases with increasing photoexcitation intensity. In particular, the amplification shows a slow response time during the light soaking from light-on to light-off condition with increasing excitation intensity in the Au/$MAPbI_3$/C_{60}/BCP/Ag device. Previous studies attributed the slow photocurrent response to the ion migration and buildup of space charges driven by electric filed.[36,46,47,48] As can be seen in **Figure 2a** this phenomenon is more dominant at higher reverse bias and photoexcitation intensity. When light is on and device is under bias both electronic and ionic charges redistribute and form new interface space charge regions, and hence develop new interfacial barrier at semiconductor/electrode interface. The interfacial charge region can't contribute to the immediate photocurrent response but can cause the slow response. Here, we observe a slow response which confirms the existing of a slow process, i.e. ion migration towards respective electrodes (**Figure 2a**). This interfacial barrier modification can trigger the injection of additional charges into the device. Hence, this slow response time provides an evidence that the current amplification is induced by optically activated ions driven by an external field. It is known that free surfaces are more susceptible to defects and surface degradation (hydration) can in fact mask the carrier transport by increasing

surface traps. This leads to resistive losses and high leakage current. Here, in **Figure 1c** and **d** we observe a small dark current which ensures the lack of leakage current. However, eventually long exposure to ambient and humidity may cause degradation in these devices.

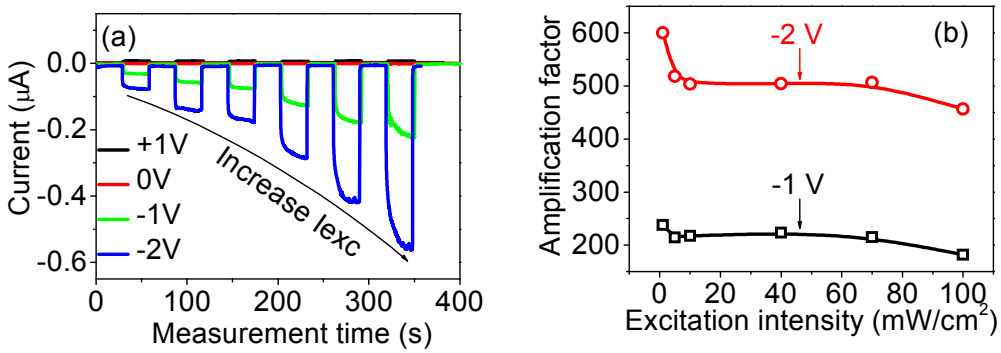

Figure 2. Excitation intensity dependence of current amplification. (a) Time-dependent current profiles measured with repeating light-on and light-off cycles with increasing excitation intensities from 1 mW/cm^2 to 100 mW/cm^2 under 0V, -1V, -2V and +1V in Au/$MAPbI_3$/C_{60}/BCP/Ag device. **(b)** The amplification factor is shown as a function of photoexcitation intensity at -1 V and -2 V.

Here, we discussed the underlying mechanism accountable for the giant current amplification in our single crystal photodetectors. As it was discussed above, the continuous illumination can cause ion migration and redistribution of charges in $MAPbI_3$ perovskite. Ion migration along a free surface or grain boundaries is easier than along bulk due to lack of chemical bonding on one side. It is revealed that photoexcitation can enhances ionic transport by changing the activation energy of ions.[49] Most recently, based on several techniques Kim *et. al*, has shown a significant ionic conduction in methyl ammonium lead iodide under illumination.[50] It was revealed that both light soaking[35] and electric field[51,52] induce halide migration and redistribution of ions in thin films and single crystals of hybrid perovskites. In addition, the drift of charged ions/vacancies towards respective contacts and compositional changes at the

electrodes was demonstrated under applied field and photoexcitation.[36,53, 54, 55] In the reverse bias regime, the Au contact is subjected to a negative bias, which can induce organic cations (MA^+) migration toward the Au contact. In our recent study, we have demonstrated that Au can interact with MA^+, forming positive complexes at the interface.[42] On the contrary, the Ag contact is subjected to a positive bias, which can induce large iodine anions (I^-) migration. With the presence of C_{60} and BCP, the I^- ions can largely accumulate at the contact interface.

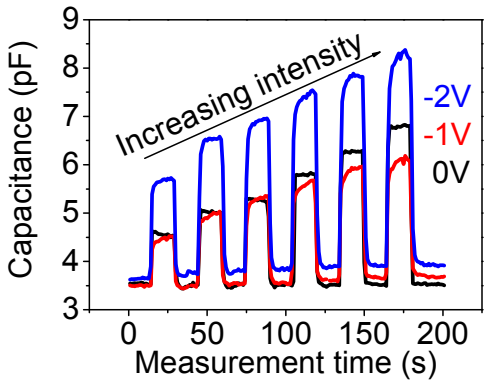

Figure 3. Time-dependent low-frequency (1 kHz) capacitance profile under different DC bias (0V, -1V and -2V) and repeating light-off/on cycles with increasing excitation intensities from 1 mW/cm^2 to 100 mW/cm^2.

To further explore the accumulation of charges at the interface we performed impedance spectroscopy. **Figure 3** presents low-frequency (1 kHz) capacitance profile monitored at different DC bias (0 V, -1 V and -2 V) with repeating light-off/on cycles. The excitation intensities are increased from 1 mW/cm^2 to 100 mW/cm^2. In general, reverse biasing is expected to assist charge dissociation, charge transport and charge collection, and consequently decrease the low-frequency capacitance, which essentially contributed from interfacial charge accumulation. The interfacial charge could have two resources: charge carriers (electrons or holes) and charged ions. When device subjected to zero bias, the capacitance profile does not

show significant time dependence, suggesting negligible ion migration under zero bias; The increment in capacitance upon increasing excitation intensity is due to the increased accumulation of charge carriers (electrons or holes). Unlikely, applying reverse bias exhibits slow response in the capacitance profile, particularly under high excitation intensity. This provides the evidence of ion migration and accumulation towards electrode interface under the manipulating of external bias and light illumination. As compared to zero bias condition, the low-frequency capacitance tends to decrease at -1 V bias but increase at -2 V. The decrease in capacitance at -1 V can be explained by the decrease in interfacial accumulation of charge carriers (electrons or holes) due to the dominant field assisted charge collection; while the increase in capacitance at -2 V is due to dominant field induced ion migration/accumulation. This interface-charge accumulation intends to reduce the internal built-in field, leading to the decrease of photovoltaic performance. However, we can expect that these accumulated ions can trigger counter charge injection from respective electrodes as shown in **Figure 4**, consequently enhancing the total current under reverse bias. Such current amplification is expected to be enhanced due to the light-assisted ion migration.[34,35]

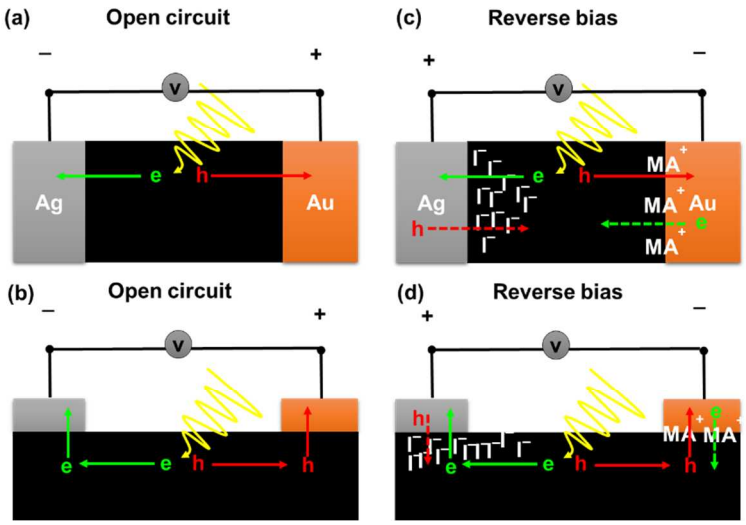

Figure 4. Proposed mechanism of the current amplification in the reverse bias regime. **(a)** Top view of open-circuit condition; **(b)** Front view of open-circuit condition; **(c)** Top view under reverse bias; **(d)** Front view under reverse bias.

In order to confirm the proposed mechanism of current amplification, we carefully measured external quantum efficiency (EQE) from our sample under different biasing conditions (0V, -0.5 V and -1 V) as shown in **Figure 5**. The original data is shown in Figure 5a, which does not consider any boundary conditions. We found that the EQE in our single crystal device is below expectations as compared to the thin film device most likely due to the large charge transport distance between the 2 electrodes (100 μm) in the lateral electrode geometry in addition to the light penetration decay in the thick single crystals (3 mm). It should be noted that the charge transport (conduction) channel between the cathode and anode has an effective thickness (x_{eff}) in a lateral geometry rather than infinity ($x_{eff}=\infty$). As a result, the EQE should be corrected by considering the effective thickness of conduction channel. **Figure 5b** plots the ratio of the number of photons absorbed within the volume with a given thickness x to that of the incident photons according to eq 3:

$$\frac{N(x)}{N_0} = e^{(-\alpha x)} \qquad (3)$$

where $N(x)$ represents the number of photons absorbed within the volume with a given thickness x, N_0 represents the number of incident photons, and $\alpha = 5 \times 10^4\ cm^{-1}$. With a rough estimation, the numbers of photons being absorbed in the effective channel is dramatically reduced to 17% and 40% when x_{eff} is taken as 50 nm and 100 nm, respectively. In addition, if the thickness (D) in a photodetector is much larger than the light penetration depth, according to (eq. 4).

$$G = \frac{n}{\tau} = \frac{\eta\frac{P_{opt}}{h\nu}}{WLD} \quad (4)$$

where P_{opt} is the incident optical power and WLD is the device dimensions, the photo-carrier generation gain decreases as the device thickness increases. By considering the effective channel thickness, EQE is indeed over unity when $x_{\text{eff}} < 100$ nm (Figure 5c and 5d).

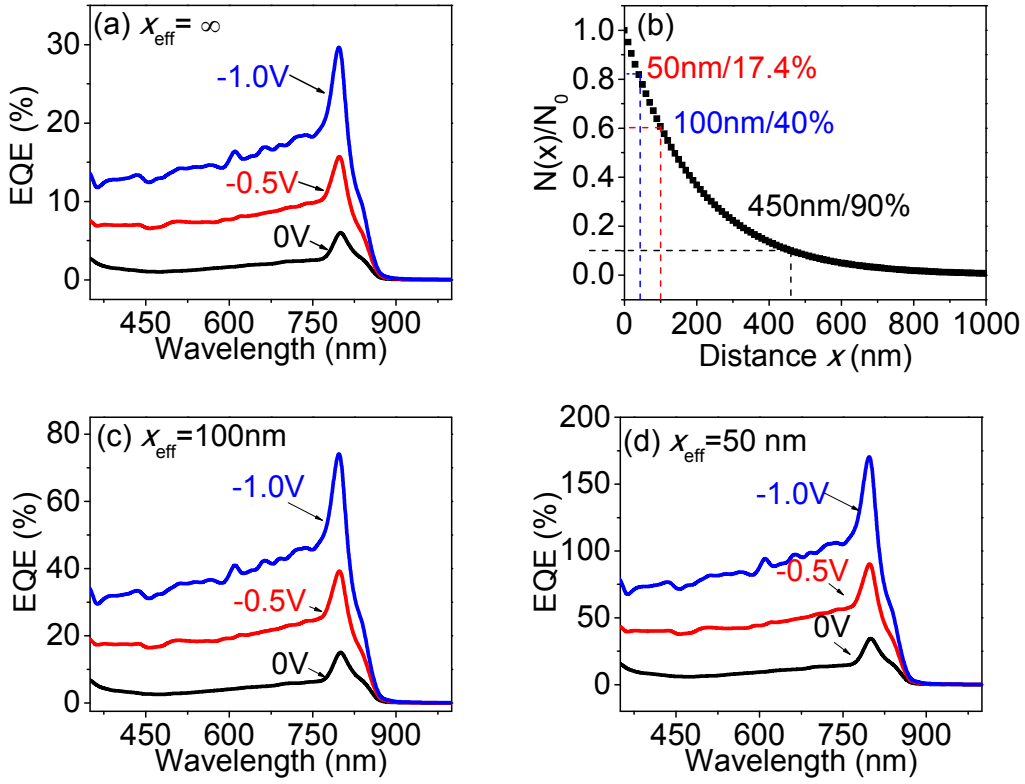

Figure 5. External quantum efficiency (EQE) of the single crystal photodetectors under different bias before and after the correction. (a) EQE of the device measured under different bias (0V, -0.5 V, and -1 V); **(b)** The ratio of the number of photons absorbed at position x to the incident photons; **(c)** EQE of the device corrected by considering the effective thickness of conducting channel (x_{eff}) of 100 nm; **(d)** EQE of the device corrected by considering x_{eff} of 50 nm.

Current amplification had been reported in both organic materials based photodetectors and polycrystalline perovskite photodetectors.[56-,58] However, the underlying mechanism remains

unsettled with the different proposed mechanisms, e.g. enhanced charge tunneling injection assisted by trapped charge carriers,[56,57] and enhanced photoconductivity due to the enhanced ferroelectric polarization.[58] Yet there are controversy on ferroelectric polarization phenomenon in hybrid perovskites. We have recently demonstrated the presence of regions with aligned electric dipoles however, ion migration, high charge mobility and free exchange between surface and bulk ionic species prevents ferroelectric switching.[59] This unique ionic and electrochemical properties of organic-inorganic perovskite open a broad range of applications beyond classical ferroelectric functionalities. For instance, they can be used as system to explore the coupling between ferroelectric and ionic behavior, i.e. recently discovered ferroionic states[60] mediated by light flux, optically-addressable gas sensors and devices for the internet of things (IoT) applications. As a result, here we rule out the ferroelectric effects as the mechanism behind this amplification. The other proposed mechanism behind photoamplification was described via modification of the potential barrier by interfacial trapped charges. The trapped charges can induce band bending at the interface, reduce the Schottky junction thickness and subsequently allow the injection of counter charges under reverse bias. In this work, the giant current amplification can be realized through the ion redistribution modifying the interfacial barrier and triggering counter carrier injection. Besides, ions on the surface of single crystals can only escape if additional energy is provided. Therefore, ions on the surface can act as trapped charges. Our proposed mechanism is similar to trap assisted charge injection in photodetectors.

CONCLUSIONS

In summary, we demonstrate a giant current amplification from the $MAPbI_3$ single crystal photodetectors with a lateral geometry of Au/$MAPbI_3$/C_{60}/BCP/Ag based on ion migration effect. A stabilized device with a light soaking for 30 mins can generate a giant amplification

with amplification factor reaching 600 at -2 V under weak light illumination (1 mW/cm^2). Such giant current amplification can be attributed to the electrical field induced migration and accumulation of ions to the respective electrodes. The interfacial charging due to ion accumulation offers an effective mechanism to trigger counter charge injection, consequently amplifying the total electrical current. Simultaneously, the field-induced ion migration wipes the defects from the working area to the electrode contacts, leading to the reduction of dark current due to the reduced density of defects within the working area. Clearly, this work provides an insightful understanding of the effect of ion migration on the photodetection action in the devices based on the single crystal of hybrid perovskites.

EXPERIMENTAL SECTION

Single crystal growth and device fabrication. The single crystals of $MAPbI_3$ were grown by solution growth method according to our previous publication.[42] Large SCs with the dimension up to sub-centimeter, were mounted on top of a glass by super glue for device fabrication. The devices were prepared with a lateral geometry of Au/$MAPbI_3$/C_{60}/BCP/Ag. The cathode and anode contacts were deposited on the crystal surface with a separation distance of 100 μm by a shallow mask. More specifically, 40 nm C_{60}, and 6 nm BCP were sequentially deposited as the electron transport layer under the vacuum of 2×10^{-7} Torr, while 100 nm Ag and 70 nm Au were deposited as cathode and anode contacts, respectively.

Measurements and characterizations. The *JV* characterizations were performed using Keithley 2400. The photoexcitation was applied by AM 1.5G solar light from Thermal Oriel 96000 300 W solar simulator. The light intensity was changed by using different neutral density filters. External quantum efficiency (EQE) spectra were measured in ambient condition using a homemade setup with a xenon arc lamp (1TDN4A, Dayton), a monochromator (CS130-RG-1-

FH, Newport), a chopper controller (SR540, Stanford Research Systems), a low-noise preamplifier (SR570, Stanford Research Systems) and a lock-in amplifier (SR830 DSP, Stanford Research Systems). The setup was calibrated with a Si detector (DET100A, Thorlabs).

ASSOCIATED CONTENT

The authors declare no competing financial interest.

AUTHOR INFORMATION

Corresponding Author

* E-mail: bhu@utk.edu

ORCID

Ting Wu: 0000-0002-2882-6547

Bin Hu: 0000-0002-1573-7625

ACKNOWLEDGMENT

This research was supported by the financial supports from Air Force Office of Scientific Research (AFOSR) under the grant number FA 9550-15-1-0064, AOARD (FA2386-15-1-4104), and National Science Foundation (CBET-1438181). This research was partially conducted at the Center for Nanophase Materials Sciences based on user projects (CNMS2016-279 and CNMS2016-R45), which is sponsored by Oak Ridge National Laboratory by the Division of Scientific User Facilities, U.S. Department of Energy. The authors also acknowledge the project support from National Science Foundation of China (Grant No. 61475051, 2014CB643506, and 2013CB922104).

REFERENCES

(1) Zhou, H.; Chen, Q.; Li, G.; Luo, S.; Song, T. B.; Duan, H. S.; Hong, Z.; You, J.; Liu, Y.; Yang, Y., Photovoltaics. Interface Engineering of Highly Efficient Perovskite Solar Cells. *Science* **2014,** *345*, 542-546.

(2) Yang, W. S.; Noh, J. H.; Jeon, N. J.; Kim, Y. C.; Ryu, S.; Seo, J.; Seok, S. I., SOLAR CELLS. High-Performance Photovoltaic Perovskite Layers Fabricated through Intramolecular Exchange. *Science* **2015,** *348*, 1234-1237.

(3) Saliba, M.; Matsui, T.; Domanski, K.; Seo, J. Y.; Ummadisingu, A.; Zakeeruddin, S. M.; Correa-Baena, J. P.; Tress, W. R.; Abate, A.; Hagfeldt, A.; Gratzel, M., Incorporation of Rubidium Cations into Perovskite Solar Cells Improves Photovoltaic Performance. *Science* **2016,** *354*, 206-209.

(4) Tan, H.; Jain, A.; Voznyy, O.; Lan, X.; Garcia de Arquer, F. P.; Fan, J. Z.; Quintero-Bermudez, R.; Yuan, M.; Zhang, B.; Zhao, Y.; Fan, F.; Li, P.; Quan, L. N.; Zhao, Y.; Lu, Z. H.; Yang, Z.; Hoogland, S.; Sargent, E. H., Efficient and Stable Solution-Processed Planar Perovskite Solar Cells *via* Contact Passivation. *Science* **2017,** *355*, 722-726.

(5) Tan, Z. K.; Moghaddam, R. S.; Lai, M. L.; Docampo, P.; Higler, R.; Deschler, F.; Price, M.; Sadhanala, A.; Pazos, L. M.; Credgington, D.; Hanusch, F.; Bein, T.; Snaith, H. J.; Friend, R. H., Bright Light-emitting Diodes Based on Organometal Halide Perovskite. *Nat. Nanotechnol.* **2014,** *9*, 687-692.

(6) Hoye, R. L.; Chua, M. R.; Musselman, K. P.; Li, G.; Lai, M. L.; Tan, Z. K.; Greenham, N. C.; MacManus-Driscoll, J. L.; Friend, R. H.; Credgington, D., Enhanced Performance in Fluorene-free Organometal Halide Perovskite Light-emitting Diodes Using Tunable, Low Electron Affinity Oxide Electron Injectors. *Adv. Mater.* **2015,** *27*, 1414-1419.

(7) Cho, H.; Jeong, S.-H.; Park, M.-H.; Kim, Y.-H.; Wolf, C.; Lee, C.-L.; Heo, J. H.; Sadhanala, A.; Myoung, N.; Yoo, S.; Im, S. H.; Friend, R. H.; Lee, T.-W., Overcoming the Electroluminescence Efficiency Limitations of Perovskite Light-emitting Diodes. *Science* **2015,** *350*, 1222-1225.

(8) Xiao, Z.; Kerner, R. A.; Zhao, L.; Tran, N. L.; Lee, K. M.; Koh, T.-W.; Scholes, G. D.; Rand, B. P., Efficient Perovskite Light-emitting Diodes Featuring Nanometre-sized Crystallites. *Nat. Photonics* **2017,** *11*, 108-115.

(9) Xing, G.; Mathews, N.; Lim, S. S.; Yantara, N.; Liu, X.; Sabba, D.; Gratzel, M.; Mhaisalkar, S.; Sum, T. C., Low-temperature Solution-Processed Wavelength-tunable Perovskites for Lasing. *Nat. Mater.* **2014,** *13*, 476-480.

(10) Zhang, Q.; Ha, S. T.; Liu, X.; Sum, T. C.; Xiong, Q., Room-temperature Near-infrared High-Q Perovskite Whispering-gallery Planar Nanolasers. *Nano lett.* **2014,** *14*, 5995-6001.

(11) Liao, Q.; Hu, K.; Zhang, H.; Wang, X.; Yao, J.; Fu, H., Perovskite Microdisk Microlasers Self-assembled from Solution. *Adv. Mater.* **2015,** *27*, 3405-3410.

(12) Zhu, H.; Fu, Y.; Meng, F.; Wu, X.; Gong, Z.; Ding, Q.; Gustafsson, M. V.; Trinh, M. T.; Jin, S.; Zhu, X. Y., Lead Halide Perovskite Nanowire Lasers with Low Lasing Thresholds and High Quality Factors. *Nat. Mater.* **2015,** *14*, 636-642.

(13) Lin, Q.; Armin, A.; Burn, P. L.; Meredith, P., Filterless Narrowband Visible Photodetectors. *Nat. Photonics* **2015,** *9*, 687-694.

(14) Xu, X.; Chueh, C.-C.; Jing, P.; Yang, Z.; Shi, X.; Zhao, T.; Lin, L. Y.; Jen, A. K. Y., High-Performance Near-IR Photodetector Using Low-bandgap $MA_{0.5}FA_{0.5}Pb_{0.5}Sn_{0.5}I_3$ Perovskite. *Adv. Func. Mater.* **2017,** *27* (28).

(15) Zhou, J. & Huang, J. Photodetectors based on Organic-inorganic Hybrid Lead Halide Perovskites. *Adv. Sci.* **2018,** *5*, 1700256-1700280.

(16) Fang, Y. J.; Dong, Q. F.; Shao, Y. C.; Yuan, Y. B.; Huang, J. S., Highly Narrowband Perovskite Single-crystal Photodetectors Enabled by Surface-charge Recombination. *Nat. Photonics* **2015,** *9*, 679-686.

(17) Saidaminov, M. I.; Adinolfi, V.; Comin, R.; Abdelhady, A. L.; Peng, W.; Dursun, I.; Yuan, M.; Hoogland, S.; Sargent, E. H.; Bakr, O. M., Planar-integrated Single-crystalline Perovskite Photodetectors. *Nat. Commun.* **2015,** *6*, 8724-8730.

(18) Bao, C.; Chen, Z.; Fang, Y.; Wei, H.; Deng, Y.; Xiao, X.; Li, L.; Huang, J., Low-noise and Large-linear-dynamic-range Photodetectors based on Hybrid-perovskite Thin-single-crystals. *Adv. Mater.* **2017,** *29*, 1703209-1703216.

(19) Divitini, G.; Cacovich, S.; Matteocci, F.; Cinà, L.; Di Carlo, A.; Ducati, C., In Situ Observation of Heat-induced Degradation of Perovskite Solar Cells. *Nat. Energy* **2016,** *1*, 15012-15018.

(20) Ahmadi, M.; Wu, T.; Hu, B., A Review on Organic-inorganic Halide Perovskite Photodetectors: Device Engineering and Fundamental Physics. *Adv. Mater.* **2017,** *29*, 1605242-1605266.

(21) Wei, H.; Fang, Y.; Mulligan, P.; Chuirazzi, W.; Fang, H.-H.; Wang, C.; Ecker, B. R.; Gao, Y.; Loi, M. A.; Cao, L.; Huang, J., Sensitive X-ray Detectors Made of Methylammonium Lead Tribromide Perovskite Single Crystals. *Nat. Photonics* **2016,** *10*, 333-339.

(22) Yakunin, S.; Dirin, D. N.; Shynkarenko, Y.; Morad, V.; Cherniukh, I.; Nazarenko, O.; Kreil, D.; Nauser, T.; Kovalenko, M. V., Detection of Gamma Photons Using Solution-grown Single Crystals of Hybrid Lead Halide Perovskites. *Nat. Photonics* **2016,** *10*, 585-589.

(23) Wei, H.; DeSantis, D.; Wei, W.; Deng, Y.; Guo, D.; Savenije, T. J.; Cao, L.; Huang, J., Dopant Compensation in Alloyed $CH_3NH_3PbBr_{3-x}Cl_x$ Perovskite Single Crystals for Gamma-ray Spectroscopy. *Nat. Mater.* **2017,** *16*, 826-833.

(24) Shrestha, S.; Fischer, R.; Matt, G. J.; Feldner, P.; Michel, T.; Osvet, A.; Levchuk, I.; Merle, B.; Golkar, S.; Chen, H.; Tedde, S. F.; Schmidt, O.; Hock, R.; Rührig, M.; Göken, M.; Heiss, W.; Anton, G.; Brabec, C. J., High-Performance Direct Conversion X-ray Detectors based on Sintered Hybrid Lead Triiodide Perovskite Wafers. *Nat. Photonics* **2017,** *11*, 436-440.

(25) Dong, Q.; Fang, Y.; Shao, Y.; Mulligan, P.; Qiu, J.; Cao, L.; Huang, J., Solar cells. Electron-hole Diffusion Lengths > 175μm in Solution-grown $CH_3NH_3PbI_3$ Single Crystals. *Science* **2015,** *347*, 967-970.

(26) Shi, D.; Adinolfi, V.; Comin, R.; Yuan, M.; Alarousu, E.; Buin, A.; Chen, Y.; Hoogland, S.; Rothenberger, A.; Katsiev, K.; Losovyj, Y.; Zhang, X.; Dowben, P. A.; Mohammed, O. F.; Sargent, E. H.; Bakr, O. M., Low Trap-state Density and Long Carrier Diffusion in Organolead Trihalide Perovskite Single Crystals. *Science* **2015,** *347*, 519-522.

(27) Liu, Y.; Yang, Z.; Cui, D.; Ren, X.; Sun, J.; Liu, X.; Zhang, J.; Wei, Q.; Fan, H.; Yu, F.; Zhang, X.; Zhao, C.; Liu, S. F., Two-inch-sized Perovskite $CH_3NH_3PbX_3$ (X = Cl, Br, I) Crystals: Growth and Characterization. *Adv. Mater.* **2015,** *27*, 5176-5183.

(28) Saidaminov, M. I.; Abdelhady, A. L.; Murali, B.; Alarousu, E.; Burlakov, V. M.; Peng, W.; Dursun, I.; Wang, L.; He, Y.; Maculan, G.; Goriely, A.; Wu, T.; Mohammed, O. F.; Bakr, O. M., High-quality Bulk Hybrid Perovskite Single Crystals within Minutes by Inverse Temperature Crystallization. *Nat. Commun.* **2015**, *6*, 7586-7591.

(29) Mizusaki, J., Arai, K. & Fueki, K. Ionic-conduction of the Perovskite-type Halides. *Solid State Ionics* **1983,** *11*, 203-211.

(30) Yang, T. Y., Gregori, G., Pellet, N., Gratzel, M. & Maier, J. The Significance of Ion Conduction in a Hybrid Organic-inorganic Lead-iodide-based Perovskite Photosensitizer. *Angew. Chem. Int. Ed.* **2015,** *54*, 7905-7910.

(31) Eames, C.; Frost, J. M.; Barnes, P. R.; O'Regan, B. C.; Walsh, A.; Islam, M. S., Ionic Transport in Hybrid Lead Iodide Perovskite Solar Cells. *Nat. Commun.* **2015,** *6*, 7497-7504.

(32) Yuan, Y. & Huang, J. Ion Migration in Organometal Trihalide Perovskite and its Impact on Photovoltaic Efficiency and Stability. *Acc. Chem. Res.* **2016,** *49*, 286-293.

(33) Back, H.; Kim, G.; Kim, J.; Kong, J.; Kim, T. K.; Kang, H.; Kim, H.; Lee, J.; Lee, S.; Lee, K., Achieving Long-term Stable Perovskite Solar Cells *via* Ion Neutralization. *Energy Environ. Sci.* **2016,** *9*, 1258-1263.

(34) Deng, Y. H., Xiao, Z. G. & Huang, J. S. Light-induced Self-poling Effect on Organometal Trihalide Perovskite Solar Cells for Increased Device Efficiency and Stability. *Adv. Energy Mater.* **2015,** *5*, 1500721-1500727.

(35) deQuilettes, D. W.; Zhang, W.; Burlakov, V. M.; Graham, D. J.; Leijtens, T.; Osherov, A.; Bulovic, V.; Snaith, H. J.; Ginger, D. S.; Stranks, S. D., Photo-induced Halide Redistribution in Organic-inorganic Perovskite Films. *Nat. Commun.* **2016,** *7*, 11683-11691.

(36) Xiao, Z.; Yuan, Y.; Shao, Y.; Wang, Q.; Dong, Q.; Bi, C.; Sharma, P.; Gruverman, A.; Huang, J., Giant Switchable Photovoltaic Effect in Organometal Trihalide Perovskite Devices. *Nat. Mater.* **2015,** *14*, 193-198.

(37) Yuan, Y. B.; Chae, J.; Shao, Y. C.; Wang, Q.; Xiao, Z. G.; Centrone, A.; Huang, J. S., Photovoltaic Switching Mechanism in Lateral Structure Hybrid Perovskite Solar Cells. *Adv. Energy Mater.* **2015,** *5*, 1500615-1500622.

(38) Tress, W.; Marinova, N.; Moehl, T.; Zakeeruddin, S. M.; Nazeeruddin, M. K.; Grätzel, M., Understanding the Rate-dependent J–V Hysteresis, Slow Time Component, and Aging in $CH_3NH_3PbI_3$ Perovskite Solar Cells: The Role of A Compensated Electric Field. *Energy Environ. Sci.* **2015,** *8*, 995-1004.

(39) Li, C.; Tscheuschner, S.; Paulus, F.; Hopkinson, P. E.; Kiessling, J.; Kohler, A.; Vaynzof, Y.; Huettner, S., Iodine Migration and Its Effect on Hysteresis in Perovskite Solar Cells. *Adv. Mater.* **2016,** *28*, 2446-2454.

(40) Meloni, S.; Moehl, T.; Tress, W.; Franckevicius, M.; Saliba, M.; Lee, Y. H.; Gao, P.; Nazeeruddin, M. K.; Zakeeruddin, S. M.; Rothlisberger, U.; Graetzel, M., Ionic Polarization-Induced Current-Voltage Hysteresis in $CH_3NH_3PbX_3$ Perovskite Solar Cells. *Nat. Commun.* **2016,** *7*, 10334-10342.

(41) Shao, Y.; Fang, Y.; Li, T.; Wang, Q.; Dong, Q.; Deng, Y.; Yuan, Y.; Wei, H.; Wang, M.; Gruverman, A.; Shield, J.; Huang, J., Grain Boundary Dominated Ion Migration in Polycrystalline Organic–inorganic Halide Perovskite Films. *Energy Environ. Sci.* **2016,** *9*, 1752-1759.

(42) Wu, T.; Mukherjee, R.; Ovchinnikova, O. S.; Collins, L.; Ahmadi, M.; Lu, W.; Kang, N. G.; Mays, J. W.; Jesse, S.; Mandrus, D.; Hu, B., Metal/Ion Interactions Induced p-i-n Junction in Methylammonium Lead Triiodide Perovskite Single Crystals. *J. Am. Chem. Soc.* **2017,** *139*, 17285-17288.

(43) Brenes, R.; Guo, D.; Osherov, A.; Noel, N. K.; Eames, C.; Hutter, E. M.; Pathak, S. K.; Niroui, F.; Friend, R. H.; Saiful Islam, M.; Snaith, H. J.; Bulović, V.; Savenije, T. J.; Stranks, S. D. Metal Halide Perovskite Polycrystalline Films Exhibiting Properties of Single Crystals. *Joule* **2017**, 1, 155 - 167

(44) Shi, J.; Xu, X.; Li, D.; Meng, Q., Interfaces in Perovskite Solar Cells. *Small*, **2015**, 11: 2472-2486.

(45) Zhao, C.; Chen, B.; Qiao, X.; Luan, L.; Lu, K.; Hu, B., Revealing Underlying Processes Involved in Light Soaking Effects and Hysteresis Phenomena in Perovskite Solar Cells. *Adv. Energy Mater.* **2015,** *5,* 1500279-1500285.

(46) Leijtens, T.; Hoke, E. T.; Grancini, G.; Slotcavage, D. J.; Eperon, G. E.; Ball, J. M.; De Bastiani, M.; Bowring, A. R.; Martino, N.; Wojciechowski, K.; McGehee, M. D.; Snaith, H. J.; Petrozza, A., Mapping Electric Field-Induced Switchable Poling and Structural Degradation in Hybrid Lead Halide Perovskite Thin Films. *Adv. Energy Mater.* **2015**, 5 (20), n/a-n/a.

(47) Azpiroz, J. M.; Mosconi, E.; Bisquert, J.; De Angelis, F., Defect migration in methylammonium lead iodide and its role in perovskite solar cell operation. *Energy & Environmental Science* **2015,** *8* (7), 2118-2127.

(48) Eames, C.; Frost, J. M.; Barnes, P. R. F.; O'Regan, B. C.; Walsh, A.; Islam, M. S., Ionic transport in hybrid lead iodide perovskite solar cells. *Nature Comm*. **2015**, 6, 7497.

(49) Zhao, Y.-C.; Zhou, W.-K.; Zhou, X.; Liu, K.-H.; Yu, D.-P. ; Zhao, Q., Quantification of light-enhanced ionic transport in lead iodide perovskite thin films and its solar cell applications *Light: Science & Applications* **2017**, 6, e16243.

(50) Kim, G. Y.; Senocrate, A.; Yang, T.-Y.; Gregori, G.; Grätzel, M.; Maier, J. Large tunable photoeffect on ion conduction in halide perovskites and implications for Photodecomposition. *Nature Mater*. **2018**, doi:10.1038/s41563-018-0038-0

(51) Luo, Y.; Khoram, P.; Brittman, S.; Zhu, Z.; Lai, B.; Ping Ong, S.; Garnett, E. C.; Fenning D. P. Direct Observation of Halide Migration and its Effect on the Photoluminescence of Methylammonium Lead Bromide Perovskite Single Crystals. *Adv. Mater*. **2017**, 29, 1703451.

(52) Vashishtha, P.; Halpert, J. E., Field-Driven Ion Migration and Color Instability in Red-Emitting Mixed Halide Perovskite Nanocrystal Light-Emitting Diodes. *Chem. Mater.* 2017, 29 (14), 5965-5973.

(53) Ding, J.; Jing, L.; Cheng, X.; Zhao, Y.; Du, S.; Zhan, X.; Cui H. Design Growth of $MAPbI_3$ Single Crystal with (220) Facets Exposed and Its Superior Optoelectronic Properties. *J. Phys. Chem. Lett*., **2018**, 9 (1), 216–221.

(54) Cheng, X.; Jing, L.; Zhao, Y.; Du, S.; Ding, J.; Zhou T. Crystal orientation-dependent optoelectronic properties of $MAPbCl_3$ single crystals. *J. Mater. Chem. C*, **2018**, 6, 1579-1586.

(55) Ding, J.; Cheng, X.; Jing, L.; Zhou, T.; Zhao, Y.; Du, S. Polarization-Dependent Optoelectronic Performances in Hybrid Halide Perovskite $MAPbX_3$ (X = Br, Cl) Single-Crystal Photodetectors. *ACS Appl. Mater. Interfaces*, **2018**, 10 (1), 845–850.

(56) Moehl, T.; Im, J. H.; Lee, Y. H.; Domanski, K.; Giordano, F.; Zakeeruddin, S. M.; Dar, M. I.; Heiniger, L. P.; Nazeeruddin, M. K.; Park, N. G.; Gratzel, M., Strong Photocurrent Amplification in Perovskite Solar Cells with A Porous TiO_2 Blocking Layer under Reverse Bias. *J. Phys. Chem. Lett.* **2014,** *5*, 3931-3936.

(57) Li, L.; Zhang, F.; Wang, J.; An, Q.; Sun, Q.; Wang, W.; Zhang, J.; Teng, F., Achieving EQE of 16,700% in P3HT:$PC_{71}BM$ based Photodetectors by Trap-assisted Photomultiplication. *Sci. Rep.* **2015,** *5*, 9181-9187.

(58) Chen, H. W.; Sakai, N.; Jena, A. K.; Sanehira, Y.; Ikegami, M.; Ho, K. C.; Miyasaka, T., A Switchable High-sensitivity Photodetecting and Photovoltaic Device with Perovskite Absorber. *J. Phys. Chem. Lett.* **2015,** *6*, 1773-1779.

(59) Ahmadi, M.; Collins, L.; Puretzky, A.; Zhang, J.; Keum, J. K.; Lu, W.; Ivanov, I.; Kalinin, S. V.; Hu, B. Exploring Anomalous Polarization Dynamics in Organometallic Halide Perovskites. *Adv. Mater.* **2018**, 30, 1705298.

(60) Yang, S. M.; Morozovska, A. N.; Kumar, R.; Eliseev, E. A.; Cao, Y.; Mazet, L.; Balke, N.; Jesse, S.; Vasudevan, R. K.; Dubourdieu, C.; Kalinin, S. V., Mixed electrochemical-ferroelectric states in nanoscale ferroelectrics. *Nat. Phys.* **2017**, 13, 812.